25th ABCM International Congress of Mechanical Engineering
October 20-25, 2019, Uberlândia, MG, Brazil

COB-2019-0818
Optimization of Heat Source Parameters in Numerical Simulations of the GTAW Welding Process of AISI 304 Butt Joints

Rodrigo Martins Farias
Louriel Oliveira Vilarinho
Universidade Federal de Uberlândia, Campus Santa Mônica, Faculdade de Engenharia Mecânica, MG, Brazil
rodrigofarias.mec@gmail.com
vilarinho@ufu.br

Paulo Roberto de Freitas Teixeira
Universidade Federal do Rio Grande (FURG), Campus Carreiros, Escola de Engenharia, RS, Brazil
prfreitasteixeira@gmail.com

Abstract. *Welding processes involve complex physical and chemical phenomena, which make mathematical modelling difficult. Several types of heat sources are available to be used in numerical simulations of welding processes. However, to get accuracy, some heat sources have many geometry parameters to be set and they demand much computational time, even using optimization methodologies. In this paper, a welding numerical analysis of a single pass butt joint weld, with square groove, of AISI 304 stainless steel, using the autogenous GTAW process is shown. The plates are 150x50x3.2 mm. Numerical simulations were performed in ANSYS® Multiphysics software, considering three types of heat sources distributions (Gaussian, Conical and Double Ellipsoid). The fusion zone shapes and thermal cycles of the plates, obtained from the experiments developed at the Laboratory of Research in Welding Processes (LAPROSOLDA – UFU), are compared with numerical results. This data, obtained by macrography and thermocouples, were used by a new optimization methodology to find the optimal parameters for these heat sources, by using the inverse problem approach and Genetic Algorithm method. Analyses of the computational time and accuracy in relation to experiments were carried out. In general, thermal results obtained by numerical simulation show good agreement with experiments. Thus, the proposed methodology strongly decreases the computational time.*

Keywords: optimization, heat source, welding, numerical simulation, reduced geometry

1. INTRODUCTION

Welds are essential parts of the engineering structures. Residual stresses and metallurgical transformations due to thermal non-linearities during welding processes can cause damage effects. An important tool to predict the behaviour of welding structures is the numerical modelling (Yaghi and Becker, 2004).

The complexity involved in welding processes requires many assumptions and approximations in numerical simulations. Although thermo-mechanical-metallurgical effects are coupled, generally, numerical simulations are carried out in sequence (thermo-mechanics or thermo-metallurgic), due to the low dependence of the thermal field in relation to others (Goldak and Akhlaghi, 2005). In the welding process, the most interesting regions in the heat transfer analysis are the fusion zone (FZ) and the heat affected zone (HAZ), where high temperatures are reached (Iacobescu, 2006). These high temperature cause phase transformations and alterations in the mechanical properties of the welded metal.

The main issue of the thermal field simulation in welding processes is the heat source modelling. Although solutions considering distributed heat sources can be reached analytically and numerically, there is an growing tendency to use numerical techniques. After Rosenthal (1941) proposed the analytical solution considering a punctual or a line heat source, several different and more realistic heat sources distributions have been developed, like the Gaussian heat source (Pavelic *et al.*, 1969), a 3D conical heat source (Balasubramanian *et al.*, 2008) (Zaeh and Schober, 2009) (Ziolkowski and Brauer, 2009), and the well known volumetric double ellipsoid distribution developed by (Goldak *et al.*, 1984), among other types of heat sources.

Finding optimal welding parameters by using experimental strategies demands many test specimens (Moradpour *et al.*, 2015) (Nagesh and Datta, 2010). Besides, there is no confidence that values are the optimal ones. However, the knowledge advance related to welding can develop considerably if welding simulations are combined with optimization techniques. This combination enables finding, computationally, optimal values of process parameters, with much less cost and time (Islam *et al.*, 2014). The computational time is the main variable that restricts a more wide use of numerical simulations

by using optimization methods. CFD simulations of welding processes, even in simple cases, can require more than 20 days (Cheon *et al.*, 2016), while simulations based on the Finite Element Method (FEM) can demand from one to more than 6 hours, depending on the mesh size and the time step (Farias *et al.*, 2016). However, optimization methods have been widely used in structural analysis based on FEM. Tajima *et al.* (2007) employed optimization techniques to investigate the optimal welding sequence that provides the lowest residual stresses. Gannon *et al.* (2010) also used an optimization technique to study the influence of the welding sequence on the distortion distribution . Fu *et al.* (2016), predicted parameters of Goldak's double ellipsoidal heat source model using optimization. Azadi Moghaddam *et al.* (2016) used the hybrid neural network and PSO in weld bead geometry. Other authors (García-García *et al.*, 2016) (Las-Casas *et al.*, 2017) have used optimization techniques, but the computational time is still high (several days).

In this work, a welding numerical analysis of a single pass butt joint weld, with square groove, of AISI 304 stainless steel, using the autogenous GTAW process is carried out. Numerical simulations were performed considering three types of heat sources. Convection and radiation on the surfaces and temperature-dependent material properties were used in the simulations. Fusion zone shapes, obtained from experiments, were used in a novel optimization methodology to determine optimal parameters of these heat sources by means of Genetic Algorithms coupled with a reduced geometry technique to diminish the computational time.

2. THEORETICAL CONCEPTS

2.1 Thermal analysis

In the welding process, phase change, with melting and solidification phenomena, is involved. Enthalpy methods are some of several techniques to deal with this type of problems. The essential feature of the basic enthalpy methods is that the evolution of the latent heat is accounted by the enthalpy as well as the relation between the enthalpy and temperature. These methods are based on the heat conduction equation expressed in function of the enthalpy as following:

$$\frac{\partial}{\partial x}(k(T)\frac{\partial T}{\partial x}) + \frac{\partial}{\partial y}(k(T)\frac{\partial T}{\partial y}) + \frac{\partial}{\partial z}(k(T)\frac{\partial T}{\partial z}) = \frac{\partial [H(T)]}{\partial t} \tag{1}$$

where *T* is the temperature, *k(T)* is the thermal conductivity, and *H* is the enthalpy, as the integral of the heat capacity with respect to temperature as following:

$$H = \int \rho(T) C_p(T) dT \tag{2}$$

where ρ is the density and C_p is the specific heat.

The thermodynamic boundary conditions on the external surfaces of the solid comprise heat transfer for convection and radiation. The heat flow density for convection (q_c) in the environment, gas or liquid, is given by Newton's heat transfer law

$$q_c = h_c(T - T_0) \tag{3}$$

where T is the temperature of the external surface, T_0 is the temperature of gas or liquid and h_c is the coefficient of convective heat transfer. This coefficient depends on the convection conditions on the solid surface, besides the properties of the surface and the environment.

The heat flow density for radiation qr is governed by the Stefan-Boltzmann law, as follows

$$q_r = \varepsilon_r \sigma_r (T^4 - T_0^4) \tag{4}$$

where ε_r is the emissivity of the material surface and σ_r is the Stefan-Boltzman constant.

2.2 Heat Sources

In this study, the heat of the welding arc was modelled by means of three different heat sources: Gaussian surface source, three-dimensional conical heat source and three-dimensional double ellipsoid heat source (Goldak and Akhlaghi, 2005). In the two-dimensional distribution of a heat source with a Gaussian distribution, the heat flux distribution on the surface of the solid is related to the radial position *r* (whose origin is the arc center), as follows (Pavelic *et al.*, 1969):

$$q(r) = \frac{\eta U I}{2\pi\sigma^2} e^{-(\frac{r^2}{2\sigma^2})} \tag{5}$$

where *q(r)* is the surface flux at radius *r*, η is the thermal efficiency, *U* is the voltage, *I* is the current and σ is the radial distance from the center.

The three-dimensional conical heat source is a volumetric heat source that considers the heat intensity distribution along the workpiece thickness. The heat intensity in the deposited region is maximum and minimum at the top and bottom surfaces of the workpiece, respectively. Along the thickness, the diameter of the heat density distribution region decreases linearly. At any plane perpendicular to z-axis, the heat intensity is distributed in a Gaussian form. At any plane perpendicular to the z-axis the heat intensity distribution may be written as

$$q(r,z) = \frac{9\eta UIe^3}{\pi(e^3-1)} \frac{1}{(z_e - z_i)(r_e^2 + r_e r_i + r_i^2)} e^{-(\frac{3r^2}{r_0^2})} \tag{6}$$

where r_0 is the distribution parameter, r is the radial coordinate, the z coordinates of the top and bottom surfaces are z_e and z_i , respectively, and radius at the top and bottom are r_e and r_i, respectively.

The three-dimensional source proposed by Goldak and Akhlaghi (2005) is a combination of two ellipses; one of them is in the front quadrant of the heat source and the other is in the rear quadrant. Equations 7 and 8 show the volumetric heat flux distributions inside the front and rear quadrants of the heat source, respectively:

$$q_r(x,y,z) = \frac{6\sqrt{3}f_r(\eta UI)}{abc_r\pi\sqrt{\pi}} e^{-3(\frac{x^2}{a^2})} e^{-3(\frac{y^2}{b^2})} e^{-3(\frac{z^2}{c_r^2})} \tag{7}$$

$$q_f(x,y,z) = \frac{6\sqrt{3}f_f(\eta UI)}{abc_f\pi\sqrt{\pi}} e^{-3(\frac{x^2}{a^2})} e^{-3(\frac{y^2}{b^2})} e^{-3(\frac{z^2}{c_f^2})} \tag{8}$$

where factors f_f and f_r are fractions of the heat imposed on front and rear quadrants, a, b, c_f and c_r are source parameters that define the size and shape of the ellipses. The Fig. 1 shows the representation of these heat sources.

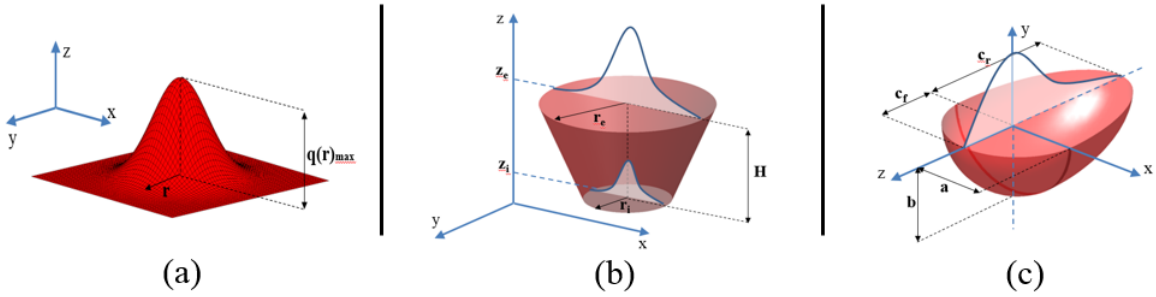

Figure 1: (a) Gaussian distribution, (b) Three-dimensional conical distribution and (c) Three-dimensional double ellipsoid distribution of a heat flux to simulate the electric arc of a welding process.

3. CASE STUDY

The case study consist in a welding process of a single pass butt joint weld, with square groove, in AISI 304 stainless steel plates. The autogenous GTAW process with Argon was used. The two plates, positioned by three tack welds, are 150x50x3.2 mm. Welding processes were carried out on a coordinate table by using a welding power supply *POWERWAVE® 455M/STT* model, from *LINCOLN®*. Three experiments were carried out with the objective of assessing the repeatability of results. Welding speed was 2mm/s and the distance from the electrode to the plate surface (DEP) was 3 mm. Voltage, current and power parameters of the welding process were acquired. The obtained voltage (RMS) was 9.4 V, the current (RMS) was 98.8 A and the instantaneous power (RMS) was 934.8 W. Both work and travel angles were 0^o. A sketch of the test is show in Fig 2.

To verify the accuracy of the methodology, in addition to the dimensions of the fused zone, thermocouple measurements were made to compare with the results obtained from the simulations. Temperatures at three points were measured by thermocouples (type K) located at the opposite face of the weld, at 3 (TC1), 8 (TC2) and 13 mm (TC3) from the weld center line, in the transverse direction. The data acquisition measurement system was the NI-9211 model (National Instruments®) with 4 samples/s/ch.

To get a better idea of the computational times, it is worth mentioning that the desktop used in the simulations has an *Intel® Core™* i5-7400 processor with 4 cores and 8 GB of RAM.

4. OPTIMIZATION METHODOLOGY

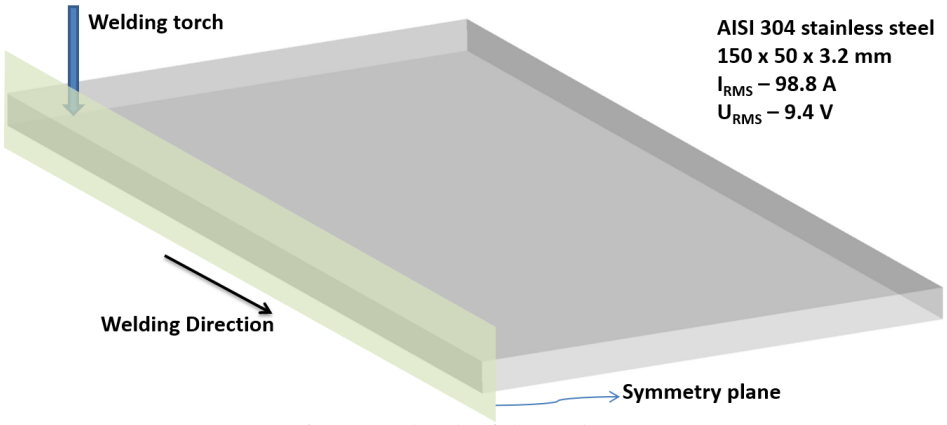

Figure 2: Sketch of the study case.

In this study, a computational methodology was developed, by means of stochastic optimization techniques (Genetic algorithms) and other specific methods, to calibrate parameters of heat sources. The flow chart of the methodology is shown in Fig 3. This methodology can be applied to several types of materials, welding processes and welded joints. The solution must be fast and capable of reproducing properly the experimental results. Besides, the methodology must consider low level of interference of the user during the optimization process.

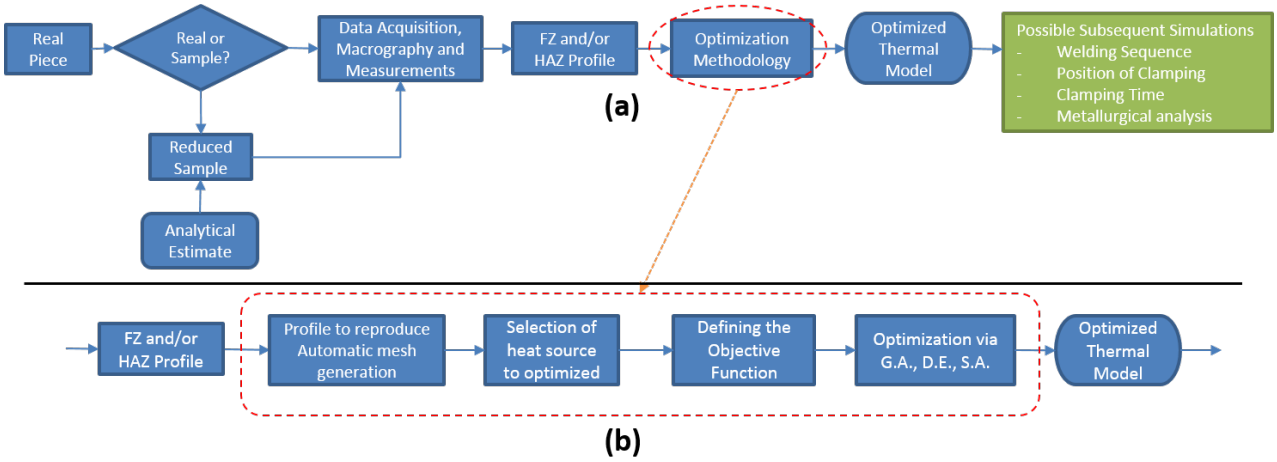

Figure 3: Flow chart of the proposed methodology: (a) process steps; (b) detail of the optimization methodology.

The available data of an experiment must be collected, such as voltage, current, dimensions of the fusion zone and/or the heat affected zone, thermocouple temperatures (if available), among others. These data are input in the model. After the choice of the type of heat source, the objective function is defined taking into account the welding geometry and/or thermal cycles. The optimization is carried out up to a optimal solution (not necessarily the global one), that respect the acceptability criterion previously established.

A technique, named Reduced Geometry, was developed to circumvent difficulties related to the computational time and to facilitate the optimization process. This technique is based on the fact that the fusion zone is a local phenomenon and distant regions do not influence it significantly. Therefore, the mesh has large element sizes in these regions that reduce considerably the mesh size and, consequently, reduce computational time. Besides, the length of the bead is also reduced, enough to have a central zone with the regime fully developed.

The optimization method described is applied to the case study. The objective is to obtain, by means of numerical simulation, the same geometry of the fusion zone of the experiment. Three points along the fusion line ($T_{solidus}$) are chose as reference. In the optimization process, temperatures of these points were used in the traditional *Least Square* function as the objective function, where a maximum value of 2700 was adopted to reach a satisfactory solution. This value represents a difference around 30^{o}C, which is 3% of the fusion temperature, in each three monitored points. The nearer the fusion temperature of the material on this points (around 1400 ^{o}C), the lower is the objective function value.

The optimization procedure was repeated three instances (for statistical assessment), with distinctive initial population, for each heat source. The thermal efficiency was additionally considered as a parameter to be optimized in the optimization procedure. Lower and upper bounds for the thermal efficiency imposed in the process were obtained from Modenesi *et al.* (2012). The evolution of 10 individuals along 20 generations was imposed as end criterion in the genetic algorithm for

all cases. Consequently, computational time of each case may be compared. However, all optimal results were obtained before the 20th generation. After the optimization using the reduced geometry, one simulation with the complete geometry is performed, with the optimal parameters obtained, to check if the same results are maintained in the complete geometry.

Table 1 shows the lower and upper bounds used for each parameter in each heat source, as well as for thermal efficiency.

Parameters	Lower Bound	Upper Bound
Thermal Efficiency (%)	50	80
Gaussian Heat Source		
σ (mm)	1.0	4.0
Conical Heat Source		
H (mm)	1.0	3.2
r_e (mm)	1.0	4.0
r_i (mm)	0.5	3.5
Goldak Heat Source		
a (mm)	0.5	4.0
b (mm)	0.5	3.2
c_f (mm)	0.5	4.0
c_r (mm)	0.5	6.0

Table 1: Bounds for the design variables used for optimization.

5. RESULTS AND DISCUSSION

The optimization process demanded a simulation time of 4.5 h on average, which is 86% lower than that obtained when the full geometry is considered, around 33 h. Table 2 presents a summary of the main results obtained from these simulations. The obtained value for the thermal efficiency for all cases stayed around 64%, what is in a good agreement with the values presented by Modenesi *et al.* (2012) and other authors.

	Gauss	Conical	Goldak
Objective function	22966	143	412
Simulation time (h)	4.4	3.9	5.3
Number of simulations	119	117	119
Thermal efficiency (%)	64.3	64.3	67.0
Generation of the optimum	13	11	19
Heat source parameters			
σ (mm)	1.16	-	-
H (mm)	-	2.22	-
r_e (mm)	-	3.57	-
r_i (mm)	-	1.84	-
a (mm)	-	-	1.57
b (mm)	-	-	0.92
c_f (mm)	-	-	3.63
c_r (mm)	-	-	3.40

Table 2: Numerical results for the optimization processes for the AISI 304 stainless steel.

Figure 4 shows the fusion zones experimentally and numerically obtained in a transverse section perpendicular to the weld, for each heat source, which presented the lowest value of the objective function. The numerical results (black dashed line) were slightly different for the Conical and the Goldak heat sources, regarding the experimental ones in terms of the fused zone (delimited by the yellow line), while the Gaussian heat source did not achieve full penetration on the joint. This can be observed in Table 2 by the high value of the objective function for this source, well above the maximum allowed value of 2700. A possible explanation for this is that the Gaussian heat source is only applied in an area, while the other two are volumetric sources, with a higher capacity to fit the shape of the fused zone.

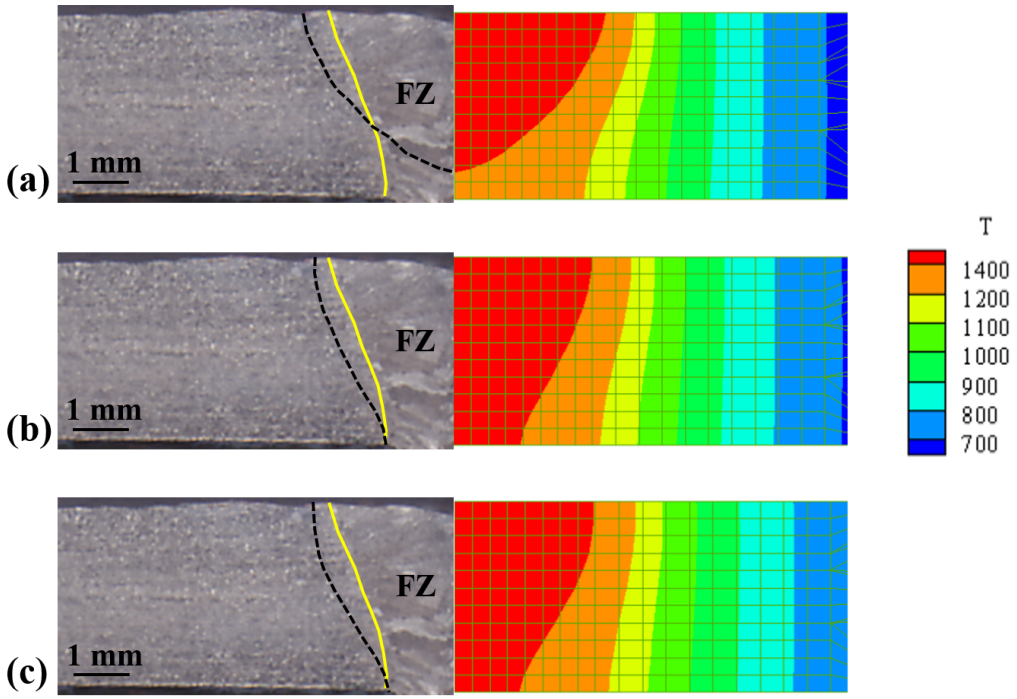

Figure 4: Experimental (left) and numerical (right) fusion zones obtained using the Gaussian (a), Conical (b) and Goldak (c) heat sources.

To verify the accuracy of the methodology, the results were also compared with thermal cycles obtained by thermocouples. Figure 5 shows the thermal cycles for TC1 thermocouple, the closest one to the weld. In general, numerical results are in good agreement with experimental ones. Regarding the peak temperatures, the results of the Goldak heat source showed the smallest difference, around 2.0% in relation to the experimental value. The slope of the temperature curve after the temperature peak represents the cooling rate, which is related to the heat transfer of the plate to the environment. In this case, the numerically obtained cooling rates are in good agreement with the experimental results. This fact leads to the conclusion that the boundary conditions, the coefficient of convective heat transfer and radiation conditions are well represented by the simulations. The differences found are mainly due to the inherent simplifications of the numerical model.

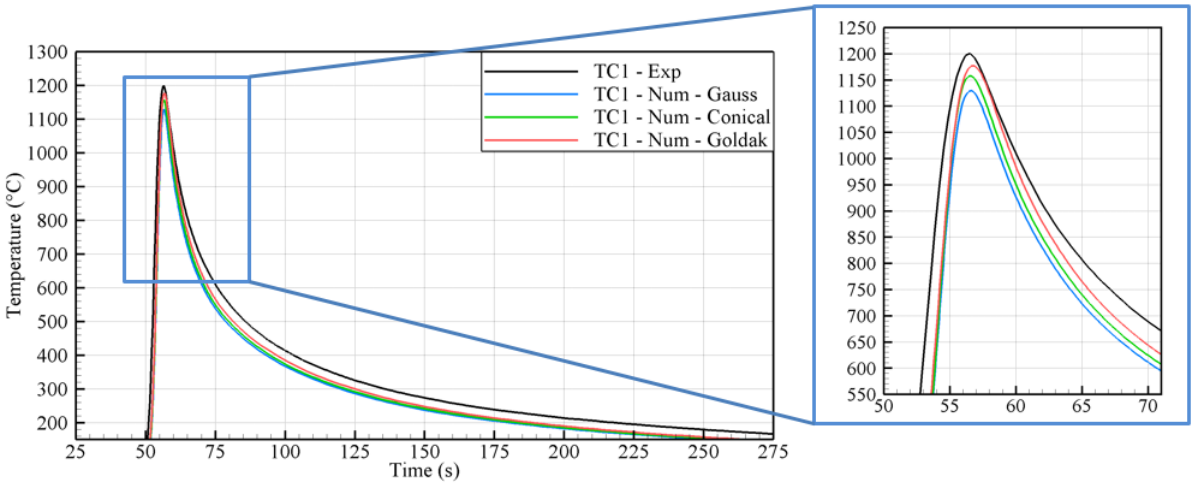

Figure 5: Experimental and numerical thermal cycles for the TC1 (3 mm) thermocouple position using the Gaussian, Conical and Goldak heat sources.

Figures 6 and 7 shows the thermal cycles for the TC2 and TC3 thermocouples, respectively. Again, in general, numerical results are in good agreement with experimental ones. Regarding the peak temperatures, the results of the Goldak heat source showed the smallest difference, around 4.0% for TC2 and 4.5% for TC3 in relation to the experimental values.

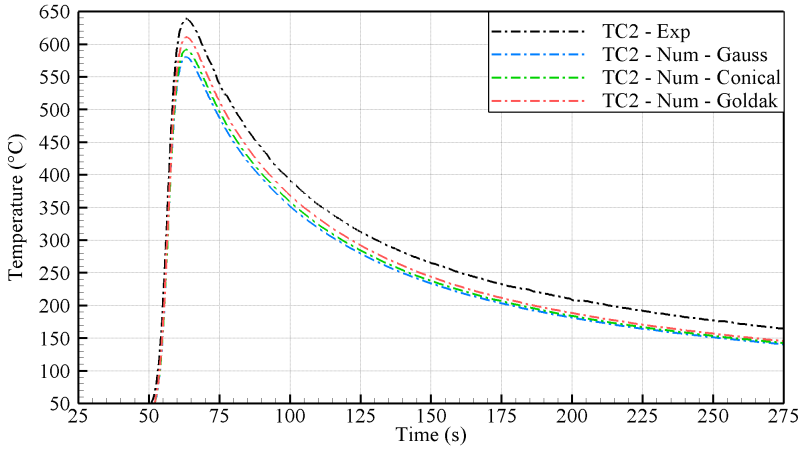

Figure 6: Experimental and numerical thermal cycles for the TC2 (8 mm) thermocouple position using the Gaussian, Conical and Goldak heat sources.

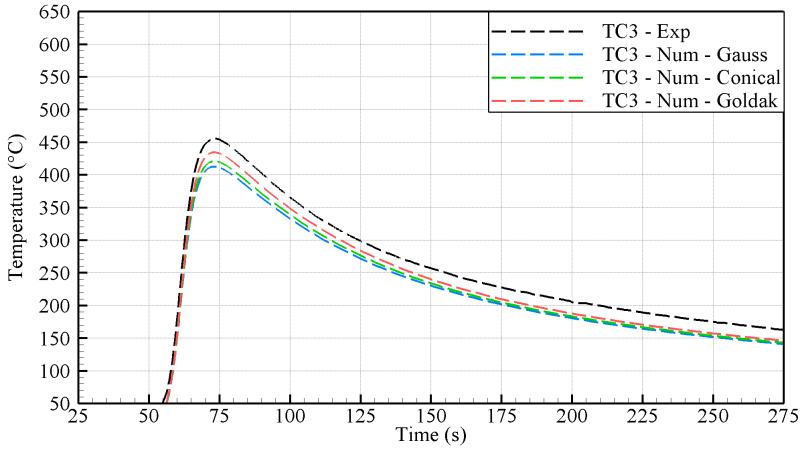

Figure 7: Experimental and numerical thermal cycles for the TC3 (13 mm) thermocouple position using the Gaussian, Conical and Goldak heat sources.

The results of the thermocouples demonstrate that the optimization of parameters of heat sources, made only with the fused zone of the welded part, is more than sufficient to approximate the numerical values to those obtained experimentally. This finding is important, especially since the use of thermocouples requires more sophisticated equipment for data acquisition and processing, while obtaining macrography data requires a simpler approach.

6. CONCLUSIONS

This paper presented a welding numerical analysis of single pass butt joint weld, with square groove, using AISI 304 stainless steel plates, of the conventional autogenous GTAW process. Numerical simulations were carried out, considering three types of moving heat sources. Fusion zone shapes, obtained from experiments, were used in a new optimization methodology to determine optimal geometric parameters of these heat sources, using a Genetic Algorithms approach. In addition, results obtained by thermocouples were also compared. Numerical results were in good agreement with experimental ones, while the proposed methodology showed that using the fusion zone as input for the optimization process presents good results for the numerical fused zone and thermal cycles, when it comes to the calibration of the parameters of these heat sources. The computational time demanded to determine the heat source parameters was, on average, 86% lower than that of a conventional simulation. In future researches, this methodology will be applied to other heat sources, welding processes and materials, such as carbon steels, aluminium alloys and other types of alloys.

7. ACKNOWLEDGEMENTS

This work was conducted during a post-graduate scholarship at the Federal University of Uberlandia, financed by the CNPq, within the Ministry of Science, Technology, Innovation and Communications of Brazil.

8. REFERENCES

Azadi Moghaddam, M., Golmezergi, R. and Kolahan, F., 2016. "Multi-variable measurements and optimization of GMAW parameters for API-X42 steel alloy using a hybrid BPNN–PSO approach". *Measurement: Journal of the International Measurement Confederation*, Vol. 92, pp. 279–287. doi:10.1016/j.measurement.2016.05.049.

Balasubramanian, K., Siva Shanmugam, N., Buvanashekaran, G. and Sankaranarayanasamy, K., 2008. "Numerical and experimental investigation of laser beam welding of aisi 304 stainless steel sheet". *Adv. Produc. Engineer. Manag*, Vol. 3, No. 2, pp. 93–105.

Cheon, J., Kiran, D.V. and Na, S.J., 2016. "Cfd based visualization of the finger shaped evolution in the gas metal arc welding process". *International Journal of Heat and Mass Transfer*, Vol. 97, pp. 1–14.

Farias, R.M., Teixeira, P.R. and Araújo, D.B., 2016. "Thermo-mechanical analysis of the mig/mag multi-pass welding process on aisi 304l stainless steel plates". *Journal of the Brazilian Society of Mechanical Sciences and Engineering*, pp. 1–14.

Fu, G., Lourenço, M.I., Duan, M. and Estefen, S.F., 2016. "Influence of the welding sequence on residual stress and distortion of fillet welded structures". *Marine Structures*, Vol. 46, pp. 30–55. doi:10.1016/j.marstruc.2015.12.001.

Gannon, L., Liu, Y., Pegg, N. and Smith, M., 2010. "Effect of welding sequence on residual stress and distortion in flat-bar stiffened plates". *Marine Structures*, Vol. 23, No. 3, pp. 385–404.

García-García, V., Reyes-Calderón, F. and Camacho-Arriaga, J.C., 2016. "Optimization of experimental temperature measurement in GTAW process by means of DoE technique and computational modeling". *Measurement: Journal of the International Measurement Confederation*, Vol. 88, pp. 297–309. doi:10.1016/j.measurement.2016.03.049.

Goldak, J., Chakravarti, A. and Bibby, M., 1984. "A New Finite Element Model for Welding Heat Sources". doi: 10.1007/BF02667333.

Goldak, J.A. and Akhlaghi, M., 2005. "Computational welding mechanics". *Springer*.

Iacobescu, G., 2006. "A theoretical model for welding process with gaussian heat source- part. 1". *University" Politehnica" of Bucharest Scientific Bulletin, Series D: Mechanical Engineering*, Vol. 68, No. 4, pp. 45–50.

Islam, M., Buijk, A., Rais-Rohani, M. and Motoyama, K., 2014. "Simulation-based numerical optimization of arc welding process for reduced distortion in welded structures". *Finite Elements in Analysis and Design*, Vol. 84, pp. 54–64.

Las-Casas, M.S., Bracarense, T.L.D., Queiroz, A. and Lima, E.J., 2017. "Weld parameter prediction using artificial neural network: FN and geometric parameter prediction of austenitic stainless steel welds". *Journal of the Brazilian Society of Mechanical Sciences and Engineering*.

Modenesi, P.J., Marques, P.V. and Santos, D.B., 2012. "Introdução á metalurgia da soldagem". Universidade Federal de Minas Gerais, Belo Horizonte, Brasil.

Moradpour, M.A., Hashemi, S.H. and Khalili, K., 2015. "Multi-objective Optimization of Welding Parameters in Submerged Arc Welding of API X65 Steel Plates". *Journal of Iron and Steel Research International*, Vol. 22, No. 9, pp. 870–878. ISSN 1006706X. doi:10.1016/S1006-706X(15)30083-2.

Nagesh, D.S. and Datta, G.L., 2010. "Genetic algorithm for optimization of welding variables for height to width ratio and application of ANN for prediction of bead geometry for TIG welding process". *Applied Soft Computing Journal*, Vol. 10, No. 3, pp. 897–907. doi:10.1016/j.asoc.2009.10.007.

Pavelic, V., Tanbakuchi, R., Uyehara, .A. and Myers, 1969. "Experimental and computed temperature histories in gas tungsten arc welding of thin plates". *Welding Journal Research Supplement*.

Rosenthal, D., 1941. "Mathematical theory of heat distribution during welding and cutting". *Welding Journal*.

Tajima, Y., Rashed, S., Okumoto, Y., Katayama, Y. and Murakawa, H., 2007. "Prediction of welding distortion and panel buckling of car carrier decks using database generated by fea". *TRANSACTIONS-JWRI*, Vol. 36, No. 1, p. 65.

Yaghi, D.A. and Becker, A., 2004. "State of the art review - weld simulation using finite element methods". Technical report, University of Nottingham, UK.

Zaeh, M.F. and Schober, A., 2009. "Approach for Modelling Process Effects during Friction Stir Welding of Composite Extruded Profiles". *Advanced Materials Research*. doi:10.4028/www.scientific.net/amr.43.105.

Ziolkowski, M. and Brauer, H., 2009. "Modelling of Seebeck effect in electron beam deep welding of dissimilar metals". *COMPEL - The International Journal for Computation and Mathematics in Electrical and Electronic Engineering*. ISSN 03321649. doi:10.1108/03321640910918940.

9. RESPONSIBILITY NOTICE

The authors are the only responsible for the printed material included in this paper.